

## Gust Response of a Supercritical Aerofoil in the Vicinity of Transonic Shock Buffet

N. F. Giannelis<sup>1</sup>, J. A. Geoghegan<sup>1</sup> and G. A. Vio<sup>1</sup>

<sup>1</sup>School of Aerospace, Mechanical and Mechatronic Engineering,  
The University of Sydney, Sydney, NSW 2006, Australia

### Abstract

Within a narrow region of the transonic flight regime, shock-wave/boundary layer interactions yield large amplitude, self-sustained shock oscillations that are detrimental to both platform handling quality and structural integrity. In this study, the aeroelastic interactions between this transonic buffet instability and a spring-suspended aerofoil are investigated by means of Reynolds-Averaged Navier-Stokes simulations. Two degree-of-freedom simulations of a supercritical aerofoil subject to a discrete gust excitation are performed at a flow state in the vicinity of the buffet instability boundary. The results show that for a small perturbation in heave, the system crosses the instability boundary and the aerodynamic and heave modes synchronise with the pitch mode. This so-called lock-in phenomenon acts a mechanism for large amplitude Limit Cycle Oscillation in aircraft structures within the transonic flow regime.

### Introduction

At certain flow conditions in the transonic flight regime, the interactions between shock waves and thin, separated boundary layers give rise to large amplitude, autonomous shock oscillations. This transonic buffet instability serves to limit the performance of aircraft. The reduced frequency of shock oscillation is typically on the order of the low-frequency structural modes, resulting in an aircraft that is susceptible to Limit Cycle Oscillation (LCO), and as a consequence, diminished handling quality and fatigue life.

Hilton & Fowler [9] first observed transonic shock-induced oscillations over six decades ago, yet the physics governing this complex phenomenon remains elusive. Lee [13] proposed an underlying mechanism based on acoustic wave propagation feedback. In Lee's model, the motion of the shock wave generates downstream propagating pressure waves, with the instability growing as it travels from the separation point through the shear layer. The separated shear layer induces a de-cambering effect, interacting with the separated flow at the trailing edge and producing pressure waves that travel upstream above the shear layer. Interaction between these upstream propagating disturbances and the shock completes a feedback loop, yielding sustained shock oscillation.

The complex shock-wave/boundary layer interactions and intermittently separated flow field inherent to the transonic buffet phenomenon pose significant challenges to numerical simulation. Further, the fundamental role of the separated flow region in Lee's [13] wave propagation feedback mechanism implies the necessity of computationally taxing scale-resolving simulations to model the instability. Nonetheless, a plethora of computational investigations have successfully captured the inherent flow features of shock-induced oscillations through Unsteady Reynolds-Averaged Navier-Stokes (URANS) methods, albeit with an appreciable sensitivity to various simulation parameters [6, 22, 7]. In particular, the selection of a suitable turbulence closure [1, 6, 23], sufficient grid refinement in the shock region [21, 10] and the use of Dual Time Stepping (DTS) with an acoustic temporal resolution [20] have been shown to be criti-

cal in URANS modelling of transonic shock buffet. Ultimately, the efficacy of URANS simulations in the prediction of transonic buffet is attributed to the low frequencies characteristic of shock motion, which exhibit significantly longer timescales than those of the shear layer eddies [22]. Such a success for a computationally efficient means of simulating intricate aerodynamic phenomena holds promise for the numerical investigation of the complex interaction mechanisms between a buffeting flow field and a deforming structure.

A number of experimental studies have considered the influence of forced harmonic motions on an aerofoil at transonic conditions [24, 3, 12]. Additionally, for harmonic excitation in the presence of shock-induced separation, a number of authors have reported aerodynamic resonance for driving frequencies near to the fundamental frequency of shock-oscillation [4, 8]. The nature of this resonance has been formalised by Raveh [17] as a frequency *lock-in* phenomenon, whereby for sufficient amplitudes of motion at excitation frequencies in the vicinity of the buffet frequency, the buffet flow response synchronises with the aerofoil motion. Raveh & Dowell [18] extended the work on shock buffet lock-in to spring-suspended aeroelastic systems, finding synchronisation of the aerodynamic and structural eigenfrequencies in pitch, heave and coupled simulations. As a significant implication of these findings, the authors propose shock buffet lock-in as a possible mechanism governing transonic LCO instabilities. More recent literature in the field has continued the exploration of aeroelastic systems in the presence of shock buffet, concentrating on classifying the influence of various structural parameters, particularly the ratio of structural and shock oscillation eigenfrequencies, on the lock-in phenomenon [5, 2, 16].

Although substantial progress has been made in understanding dynamic interactions in the presence of developed shock buffet, little research exists regarding the aeroelastic response of systems in the vicinity buffet onset. This paper seeks to explore such aeroelastic interactions at pre-buffet flow states. Static aerofoil buffet simulations for a supercritical aerofoil are performed and validated against experimental data. Dynamic computations for a pitching and heaving system are then developed, and the influence of a discrete shaped gust profile on the aeroelastic response of the aerofoil at pre-buffet conditions is quantified through time and frequency domain analysis.

### Numerical Method

#### Test Case

This study investigates the flow field around the OAT15A supercritical aerofoil at transonic buffet conditions. Experiments on this section have been performed in the S3Ch Continuous Research Wind Tunnel at the ONERA Chalais-Meudon Centre and are detailed by Jacquin et. al. [11]. A wind tunnel model of 12.3% relative thickness, 230 mm chord, 780 mm span and a 1.15 mm thick trailing edge was constructed for the experiment. The model ensured a fixed boundary layer transition at 7% chord through the installation of a carborundum strip on the upper and lower surfaces.

The experiments conducted at ONERA sought to develop an extensive experimental database for the validation of numerical buffet simulations. The model was fitted with 68 static pressure orifices and 36 unsteady Kulite pressure transducers through the central span to mitigate 3D effects from sidewall boundary layers. Adaptable upper and lower wind tunnel walls further alleviated wall interference. The investigation applied a sublimating product to the model surface, permitting oil flow visualizations for characterisation of turbulent regions and shock motion. The authors employed Schlieren imaging and Laser Doppler Velocimetry (LDV) to qualitatively characterise buffet flow features. Further, steady and unsteady pressure measurements permitted the collection of mean and RMS pressure data, along with spectral content for the pressure fluctuations.

The test programme undertaken by Jacquin et. al. [11] consisted of an angle of attack sweep at  $M_\infty = 0.73$  to obtain data for buffet onset, as well as Mach number sweeps at  $\alpha_\infty = 3^\circ$  and  $\alpha_\infty = 3.5^\circ$ . In this study, the data at  $M_\infty = 0.73$  and  $\alpha_\infty = 3.5^\circ$  is employed for validation of the buffet computations. The pre-buffet flow state at  $M_\infty = 0.73$  and  $\alpha_\infty = 3^\circ$  is then taken as a baseline at which the gust response is analysed.

#### Flow Solver

Simulations are performed using the commercial, cell-centred finite volume code ANSYS Fluent R16.2. The 2D density-based implicit solver is used to formulate the coupled set of continuity, momentum and energy equations. The inviscid fluxes are resolved by an upwind Roe flux difference splitting scheme with the blended central difference/second-order upwind MUSCL scheme for extrapolation of the convective quantities. All diffusive fluxes are treated with a second-order accurate central-difference scheme. Gradients for the convection and diffusion terms are constructed through a cell based Least Squares method and solved by Gram-Schmidt decomposition of the cells coefficient matrix.

For the viscous closure of the Navier-Stokes equations, Menter's  $k - \omega$  Shear Stress Transport (SST) [14] model is employed. This model has been selected based on superior prediction of mean pressure distribution, RMS pressure fluctuations, buffet amplitude and frequency, as detailed in the preceding work [5]. All turbulent transport equations are solved segregated from the coupled set of continuity, momentum and energy equations, with second-order accurate upwind discretisation of the turbulent quantities.

#### Temporal and Spatial Discretisation

Calculations in this study are performed on a two-dimensional CH-type structured grid with far-field boundaries located 80 chord lengths from the profile. The domain is divided into two zones; a laminar region upstream and along 7% of the aerofoil chord forward section and a turbulent region in the remainder of the domain to represent the experimentally imposed boundary layer transition.

Three grids have been generated to assess mesh independence, with the grid parameters provided in table 1. Refinement levels are primarily dictated by shock resolution across the aerofoil surface, with minor refinement adopted in the wall normal direction. A wall  $y^+ \approx 1$  is achieved at each level of refinement. Grid convergence is assessed based upon steady flow pressure distributions at  $M_\infty = 0.73$  and  $\alpha_\infty = 3^\circ$ . Grid independent solutions are achieved with Grid B and thus, this grid is employed for all subsequent simulations. Grid B is comprised of 285 nodes along each surface of the aerofoil profile, 96 nodes in the wake and 92 nodes in the wall normal direction.

Grid	Size ( $i \times j$ )	Shock Resolution (c)
A	288 $\times$ 86	0.005
B	381 $\times$ 92	0.0035
C	472 $\times$ 98	0.0025

Table 1: Computational Grid Properties

Transient simulations are also performed to validate the numerical method's ability to predict transonic buffet phenomenon. The developed buffet condition of  $M_\infty = 0.73$  and  $\alpha_\infty = 3.5^\circ$  is considered. Whilst a complete analysis is presented in [5], the transient simulations correlate well with the experimental mean and RMS pressures. Additionally, the buffet frequency and lift differential is well captured.

#### Dynamic Aeroelastic Simulations

To investigate the aeroelastic response of the OAT15A aerofoil at a pre-buffet flow state and subject to a gust excitation, Fluent's Six-DOF Rigid Body solver is employed. For the fluid, the simulations are performed at  $M_\infty = 0.73$  and a mean  $\alpha_\infty = 3^\circ$ . For comparison of the observed structural and aerodynamic frequencies during frequency domain analysis, the static aerofoil buffet reduced frequency ( $\bar{f}_{SB_0}$ ) at onset ( $\alpha_\infty = 3.5^\circ$ ) is computed, yielding  $\bar{f}_{SB_0} = 0.43$ .

Two degree-of-freedom aeroelastic simulations are performed with the aerofoil constrained to pitch and heave motions. The computations are initialised with the steady-state solution at the pre-buffet condition. In the present study, no structural damping is considered and the aeroelastic system is modelled as a spring-mass in both pitch and heave. The equation of motion for the pitching system is thus:

$$I_\alpha(\ddot{\alpha} + \omega_\alpha^2 \alpha) = M_{1/4c} \quad (1)$$

where  $\alpha$  and  $\ddot{\alpha}$  are the pitch displacement and acceleration respectively,  $\omega_\alpha$  is the pitch natural frequency and  $M_{1/4c}$  is the pitching moment about the quarter-chord point. The elastic axis and centre of gravity are imposed to be coincident with the quarter-chord point such that all moments in equation (1) are taken about this point. The pitch moment of inertia  $I_\alpha$  is computed by:

$$I_\alpha = \mu \pi \rho_\infty b^3 r_\alpha^2 \quad (2)$$

where  $\rho_\infty$  is the freestream density,  $b$  is the aerofoil semi-chord,  $r_\alpha^2 = 0.75$  is the radius of gyration and  $\mu = 50$  is the sectional mass ratio. Similar to equation (1), the equation of heaving motion is given by:

$$m(\ddot{h} + \omega_h^2 h) = L \quad (3)$$

where  $h$  and  $\ddot{h}$  are heave displacement and acceleration respectively,  $\omega_h$  is the heave natural frequency and  $L$  is the vertical force on the aerofoil section suspended at the quarter-chord point.

As evidenced by Raveh [17] and Giannelis & Vio [5], shock buffet lock-in occurs for pitch frequencies above and heave frequencies below the fundamental buffet frequency. To investigate the potential of lock-in resulting due to a gust excitation, wind-off structural reduced frequencies of  $\bar{f}_\alpha = 1.2\bar{f}_{SB_0}$  and  $\bar{f}_h = 0.8\bar{f}_{SB_0}$  are imposed for the pitch and heave modes, respectively. Such a configuration is representative of a dynamic aeroelastic system comprised of first wing bending and first wing torsion modes. Further, to isolate the effects of gust excitation, both the linear and torsional springs are pre-stressed such that the computations are initialised at a static aeroelastic equilibrium.

## Gust Modelling

The gust excitation is modelled through the quasi-static, 1-cosine shaped gust profile of Pratt & Walker [15]. The gust load is deterministic and assumes a vertical disturbance with a small magnitude relative to the freestream velocity. Consequently, the discrete gust velocity acts to increase the effective angle of attack, and as will be shown, trigger the transonic buffet instability and the associated lock-in phenomenon.

The gust excursion is implemented through a time dependent incremental load applied to the heave degree-of-freedom:

$$F_g(t) = \frac{1}{2}g\Delta n\mu\pi\rho_\infty b^2 \left(1 - \cos\frac{2\pi(t-t_0)}{t_g}\right) \quad \text{for } t_0 \leq t < t_0 + t_g \quad (4)$$

where  $F_g(t)$  is the incremental vertical force at time  $t$ ,  $t_0$  is the gust start time with a gust duration of  $t_g$ . The parameter  $\Delta n$  represents the incremental load factor, and is calculated in accordance with Ricciardi et. al. [19].

Simulations are run for a nondimensional time of  $\bar{t} = 1500$ , normalised with respect to acoustic velocity. The time histories of the lift coefficient and heave and pitch displacements are then extracted. Spectrograms are also constructed by Short-Time Fourier Transform (STFT) to observe the variations in frequency content during lock-in.

## Results

In figure 1, the time histories of the lift coefficient, heave displacement and pitch displacement are shown. The simulations are seen to begin from a static aeroelastic equilibrium, evident in the steady response for  $\bar{t} < 100$ . At  $\bar{t} = 100$ , the gust excitation is applied to the heave mode, resulting in a peak heave displacement of 1.6 mm ( $< 0.01c$ ) in figure 1(b). From this small perturbation in heave, the pitch mode is excited and is seen to begin oscillations in figure 1(c). A small transient period then ensues for  $100 < \bar{t} < 250$ , where the heave mode and lift coefficient oscillate periodically at the heave fundamental frequency. During this period, the pitch mode in figure 1(c) is seen to exhibit aperiodic oscillations. Between  $250 < \bar{t} < 400$ , aperiodic oscillations also appear in the lift coefficient, and for  $\bar{t} > 400$ , the amplitude of the lift coefficient and pitch displacement steadily increases, culminating in large amplitude LCOs at  $\bar{t} = 750$  which are characteristic of shock buffet lock-in. During this time, the heave mode experiences a transient response, transitioning to a low amplitude, high frequency LCO.

Further insight into the lock-in phenomenon is achieved by considering the change in frequency content of the aerodynamic and structural responses over time. In figure 2, the spectrograms of the lift, heave and pitch histories are given where  $f_{SB}$ ,  $f_h$  and  $f_\alpha$  represent the lift, heave and pitch response frequencies, respectively. In figure 2(b), the vertical gust excitation is evident in the broadband frequency content in the heave response for  $\bar{t} < 250$ . The heave excitation is sufficient to incite a dynamic lift response in figure 2(a), where the frequency content is initially concentrated at the heave natural frequency. As the simulation progresses, the dominant frequency of the lift response migrates to the pitch eigenfrequency. As  $\bar{t} > 900$ , the aerodynamic response has synchronised completely with the pitch mode, with frequency content also evident at the first two pitch superharmonics. The heave motion also synchronises with the pitch mode, however, convergence occurs only after a significant transient where both the pitch and heave frequencies are prevalent. The heave perturbation is further evident in the frequency content of the pitching motion in figure 2(c). The vertical displacement of  $< 0.01c$  is sufficient to excite the pitch

mode, and as the time dependent aerodynamic loads drive the pitching motion, the frequency content migrates quickly to the pitch eigenfrequency. At this point, an aerodynamic resonance ensues and with sufficient pitch displacement, the aeroelastic system crosses the buffet instability boundary. As the aerodynamic and pitch modes synchronise, lock-in occurs and large amplitude LCOs develop.

## Conclusions

In this paper, transonic flow over the supercritical OAT15A aerofoil has been investigated through URANS simulation at developed and pre-buffet conditions. The static aerofoil computations are validated against experimental data and are able to reproduce the flow features inherent to transonic buffet. The aeroelastic simulations indicate that at pre-buffet conditions a small perturbation, represented by a discrete vertical gust, is sufficient to incite the transonic shock buffet instability. For the particular combination of parameters investigated, the aerodynamic response exhibits lock-in to the pitch mode, yielding large amplitude aerodynamic and pitch LCOs. The potential of these substantial aerodynamic and structural oscillations to develop at pre-buffet flow states may have significant implications for the certification of aircraft. Further study is required to quantify precisely how near to the instability boundary an aircraft system may exist, such that regulation gust loads do not produce a detrimental aeroelastic response.

## Acknowledgements

This research was partially funded by the Defence Science and Technology Group, Australia.

## References

- [1] Barakos, G. and Drikakis, D., Numerical Simulation of Transonic Buffet Flows using various Turbulence Closures, *International Journal of Heat and Fluid Flow*, **21**, 2000, 620–626.
- [2] Carrese, R., Marzocca, P., Levinski, O. and Joseph, N., Investigation of Supercritical Airfoil Dynamic Response due to Transonic Buffet, *Proceedings of the 54th AIAA Aerospace Sciences Meeting* AIAA Paper 2016-1552, San Diego, CA, January 2016.
- [3] Davis, S., NACA 64A010 Oscillatory Pitching, *Compendium of Unsteady Aerodynamics Measurements* AGARD-R-702, 1982, 46–67.
- [4] Davis, S. and Malcolm, G., Transonic shock-wave/boundary-layer interactions on an oscillating airfoil, *AIAA Journal*, **18**, 1980, 1306–1312.
- [5] Giannelis, N. and Vio, G., Aeroelastic Interactions of a Supercritical Aerofoil in the Presence of Transonic Shock Buffet, *Proceedings of the 54th AIAA Aerospace Sciences Meeting* AIAA Paper 2016-2028, San Diego, CA, January 2016.
- [6] Goncalves, E. and Houdeville, R., Turbulence model and numerical scheme assessment for buffet computations, *International Journal for Numerical Methods in Fluids*, **46**, 2004, 1127–1152.
- [7] Grossi, F., Braza, M. and Hoarau, Y., Prediction of Transonic Buffet by Delayed Detached-Eddy Simulation, *AIAA Journal*, **52**, 2014, 2300–2312.

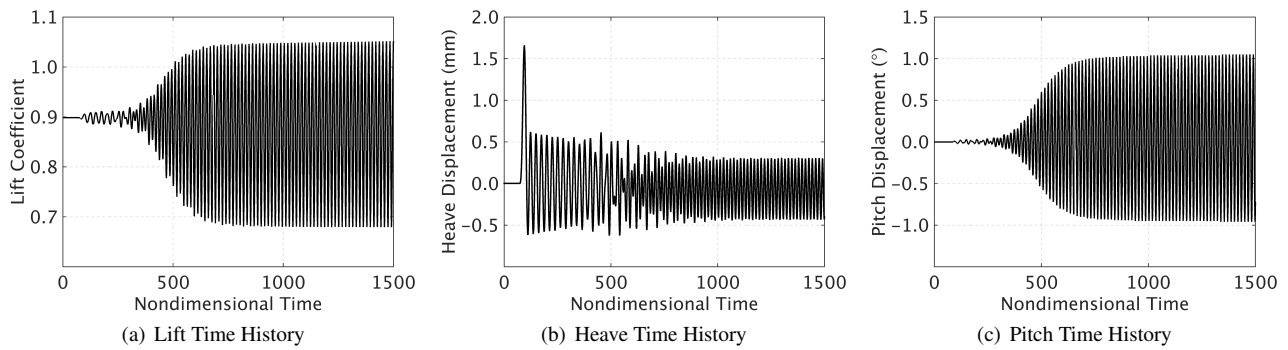


Figure 1: Time Histories of the Lift Coefficient, Heave Displacement and Pitch Displacement

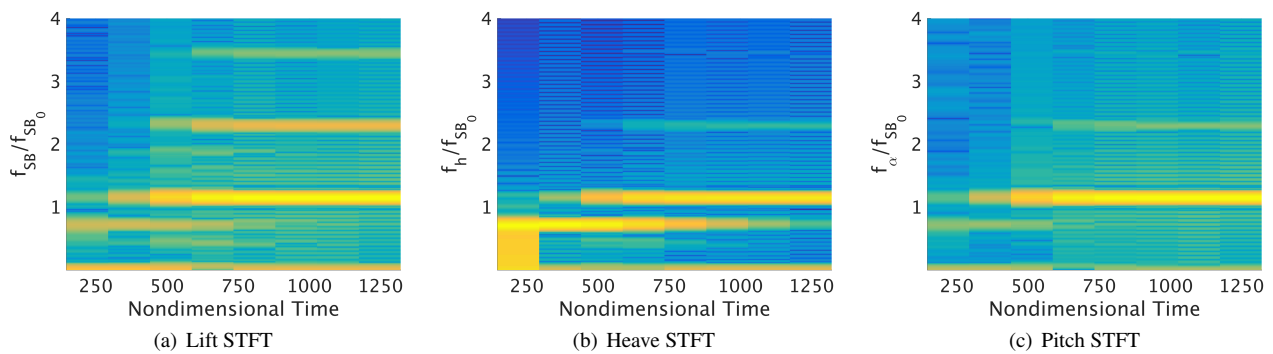


Figure 2: Short-Time Fourier Transforms of the Lift, Heave and Pitch Time Histories

- [8] Hartmann, A., Klaas, M. and Schröder, W., Coupled airfoil heave/pitch oscillations at buffet flow, *AIAA Journal*, **51**, 2013, 1542–1552.
- [9] Hilton, W. and Fowler, R., Photographs of shock wave movement, NPL R&M No. 2692, National Physical Laboratories, December 1947.
- [10] Iovnovich, M. and Raveh, D., Reynolds–Averaged Navier–Stokes Study of the Shock–Buffet Instability Mechanism, *AIAA Journal*, **50**, 2012, 880–890.
- [11] Jacquin, L., Molton, P., Deck, S., Maury, B. and Soulevant, D., Experimental Study of Shock Oscillation over a Transonic Supercritical Profile, *AIAA Journal*, **47**, 2009, 1985–1994.
- [12] Landon, R., NACA 0012 Oscillatory and Transient Pitching, *Compendium of Unsteady Aerodynamics Measurements* AGARD-R-702, 1982, 68–92.
- [13] Lee, B., Self-Sustained Shock Oscillations on Airfoils at Transonic Speeds, *Progress in Aerospace Sciences*, **37**, 2001, 147–196.
- [14] Menter, F., Two-equation eddy-viscosity turbulence models for engineering applications, *AIAA Journal*, **32**, 1994, 1598–1605.
- [15] Pratt, K. and Walker, W., A Revised Gust-Load Formula and a Reevaluation of V-G Data Taken on Civil Transport Airplanes from 1933 to 1950, NACA Report 1206, 1954.
- [16] Quan, J., Zhang, W., Gao, C. and Ye, Z., Characteristic analysis of lock-in for an elastically suspended airfoil in transonic buffet flow, *Chinese Journal of Aeronautics*, **29**, 2016, 129–143.
- [17] Raveh, D., Numerical Study of an Oscillating Airfoil in Transonic Buffeting Flows, *AIAA Journal*, **47**, 2009, 505–515.
- [18] Raveh, D. and Dowell, E., Aeroelastic responses of elastically suspended airfoil systems in transonic buffeting flows, *AIAA Journal*, **52**, 2014, 926–934.
- [19] Ricciardi, A. P., Patil, M. J., Canfield, R. A. and Lindsley, N., Evaluation of quasi-static gust loads certification methods for high-altitude long-endurance aircraft, *Journal of Aircraft*, **50**, 2013, 457–468.
- [20] Rouzaud, O., Plot, S. and Couaillier, V., Numerical simulation of buffeting over airfoil using dual time stepping method, *Proceedings of ECCOMAS 2000*, Barcelona, Spain, September, 2000.
- [21] Rumsey, C., Sanetrik, M., Biedron, R., Melson, N. and Parlette, E., Efficiency and accuracy of time-accurate turbulent navier-stokes computations, *Computers & Fluids*, **25**, 1996, 217–236.
- [22] Sartor, F., Mettot, C. and Sipp, D., Stability, Receptivity, and Sensitivity Analyses of Buffeting Transonic Flow over a Profile, *AIAA Journal*, **53**, 2014, 1980–1993.
- [23] Thiery, M. and Coustols, E., URANS computations of shock-induced oscillations over 2D rigid airfoils: Influence of test section geometry, *Flow, Turbulence and Combustion*, **74**, 2005, 331–354.
- [24] Tijdeman, H., *Investigations of the transonic flow around oscillating airfoils*, PhD Thesis, TU Delft, Delft University of Technology, 1977.